Korean J. Chem. Eng., 39(7), 1919-1926 (2022)
DOI: 10.1007/s11814-022-1115-2

pISSN: 0256-1115
eISSN: 1975-7220

High potential of amine rice husk magnetic biocomposites for Cu(II) ion adsorption and heterogeneous degradation of contaminants in aqueous solution

Iryanti Fatyasari Nata*,,†, Doni Rahmat Wicakso*, Agus Mirwan*, Chairul Irawan*, Rinna Juwita*, Niken Anggraini Astuti*, and Rizka Tiara An-Nisa***

*Department of Chemical Engineering, Lambung Mangkurat University, Banjarbaru, South Kalimantan 70714, Indonesia
**Wetland-based Materials Research Centre, Lambung Mangkurat University, Banjarbaru, 70714 Indonesia
(*Received 18 September 2021 • Revised 2 March 2022 • Accepted 15 March 2022*)

Abstract−Rice husk (RH) cellulose as a matrix was synthesized for amine rice husk magnetic biocomposite (RB-NH_2) by one-pot solvothermal method. The synergic effect of amine on magnetic nanoparticle will enhance the reactivity of material. Ethylene glycol as solvent was used for dissolved iron(III) chloride hexahydrate, Na-acetate anhydrate, and 1,6-hexanediamine, then RH was added, kept at ±200 °C for 6 h. The optimums of Fe contained and amine concentrations on biocomposite were detected at 93% and 2.9 mmol/g, respectively. The surface area of rice husk significantly increased from 1.309 m^2 g^{-1} to 19.45 m^2 g^{-1} when converted to biocomposite. The RB-NH_2 has good capability to adsorb Cu(II) ion at 116.45 mg g^{-1} at pH 5 for 60 min. Surprisingly, during adsorption, the RB-NH_2 also worked on reducing the chemical oxygen demand (COD) number, total suspended solid (TSS) and dye for 22%, 54.37%, and 33.74%, respectively. The reuse effectiveness for RB-NH_2 showed a good result with four repetitions. The multiple effects of amine rice husk magnetic biocomposite on wastewater contaminants leads to becoming a candidate material to be developed and applied in a wide range of waste water treatment applications.

Keywords: Adsorption, Biocomposite, Cu(II) Ion, Magnetic, Rice Husk, Solvothermal

INTRODUCTION

Rice husk is a by-product of rice milling and is only used as fuel for brick burning, cooking or just throwing it away [1]. Improper handling of rice husks will cause pollution to the environment. Rice husk as waste agriculture process consists of lignocellulose, which causes strong and rigid properties, especially for cellulose around 31-49% [2]. Based on these stiff and strong properties, rice husk has potential for composite raw material [3]. The utilization of rice husk carbon (RH-C) was investigated for carbon black [4], isolation of silica [5], dye removal [6], and metal ion adsorption [7]. Nowadays, magnetic properties are widely used in several applications, as well as silicon steel [8], drug delivery [9], antimicrobial [10] and as adsorbent for metal ions [11]. The property of magnetism has advantage for specific applications. Synthesis of magnetic nanoparticle (MNPs) using solvothermal method produced high quality MNPs: stable, uniform particle size and a high degree of magnetification so that they have the potential to be developed as adsorbents [12]. The advantage of using waste of biomass as raw material is that it is in nature and covers the environment problem. Nanotechnology research in the environmental field, especially the prevention of heavy metal pollution, pays great attention to nanoparticle-based adsorbents because they have been proven to be able to overcome water pollution by heavy metals. Adsorption is a widely used method in the removal of heavy metals because of its efficiency and easy operation. The adsorbent commonly used is nanoparticle-based adsorbent [13], with particle size in the nanometer scale it has a high surface area that can absorb many metals; therefore, nanoparticles are very suitable to be used as metal adsorbent [14].

To improve the quality and functionality of materials, are many researches have modified the material for heavy metal ion adsorption [15] and other contaminants such as ampicillin [16], oil spill remediation [17], and other pollutants [18]. Although tiny amounts of copper Cu(II) are essential for human health, excess amounts can cause adverse health effects, including nausea and gastrointestinal problems [19]. However, they are still limited to observing the optimum parameter condition for Cu(II) ion adsorption and heterogeneous degradation of other contaminants by one step reaction. Especially for textile industry wastewater, it contains total suspended solid (TSS), chemical oxygen demand (COD) and dye. Based on our previous research [7,20], the amine functionalized on rice husk magnetic biocomposite has good capability to adsorb Fe(III) ion and Pb(II) ion.

In this study, the characterization of amine rice husk magnetic biocomposite was observed to approve the properties of material as biocomposite. The biocomposite was applied as adsorbent for Cu(II) ion removal. The kinetic study for adsorption, performance to degrade of TSS, COD and dye in wastewater was also investigated. In order to evaluate the effect amine surface functionalization, the biocomposite without amine functionalization was also used as adsorbent in the same condition. The results are expected to increase the capability of biocomposite as adsorbent and can resolve more contaminants of wastewater in the environment.

†To whom correspondence should be addressed.
E-mail: ifnata@ulm.ac.id

MATERIALS AND METHODS

1. Materials

Rice husk (RH) was obtained in Gambut, South Kalimantan, Indonesia. The Sarangani textile industry from Cempaka District, Banjarbaru, South Kalimantan was chosen as sample for adsorption. Copper (II) chloride ($CuCl_2$), ethylene glycol ($C_2H_6O_2$), anhydrous sodium acetate ($C_2H_3NaO_2$), iron (III) chloride hexahydrate ($FeCl_3{\cdot}6H_2O$), 1,6-hexanediamine ($C_6H_{16}N_2$), sodium hydroxide (NaOH), hydrochloric acid (HCl), ethanol (C_2H_5OH) were purchased from Sigma Aldrich.

2. Rice Husk Delignification

Rice husk was washed with tap water and dried in an oven at 105 °C for 7 h and crushed to become powder and pass 60 mesh sieves. Rice husk powder (40% v/v) was soaked for 2 h in 1% of NaOH solution (ASTM-D-1109-56, 1978), heated at 80 °C for 2 h and 150 rpm under stirring. After reaction, the solid part washed with deionized (DI) water until pH of filtrate was neutral. The solid part was dried in an oven at 105 °C for 7 h and the material was called RH-D. The RH was delignified to remove lignin content and produce lignin-free cellulose fiber.

3. Synthesis of Amine Rice Husk Magnetic Biocomposite

The amine magnetic biocomposite was prepared by solvothermal method, with ethylene glycol (24 mL) as a solvent. Anhydrous sodium acetate (1.6 g), iron (III) chloride hexahydrate (0.8 g), 1,6-hexanediamine (7 mL) were put into a glass beaker, then heated at 60 °C for 15 min under stirring of 150 rpm. The RH-D (0.5 g) was added to the mixture and put in 50 mL Teflon stainless steel autoclave reactor and heated for 6 h at 200 °C. The reactor was cooled to room temperature after the process, and then the biocomposite was washed with DI water and 40% of ethanol for three times. The washing step is to remove the remaining chemical in the mixture. The biocomposite was called (RB-NH_2). The naked MNPs also was produced by same procedure above without addition of RH-D. In addition, the biocomposite without 1,6-hexanediamine (RB-M) was also produced as a control. All prepared materials were kept in DI water for future use.

4. Adsorption of Cu(II) Ion, Total Suspended Solid (TSS), and Chemical Oxygen Demand (COD) onto Amine Magnetic Rice Husk Biocomposite

A batch adsorption experiment of Cu(II) ion was carried out to determine the adsorption capacity of biocomposite using wastewater of Sarangani textile industry. The contact time and pH (4, 5, and 6) effect of solution were studied in the adsorption process comprehensively. A weighed amount of biocomposite was added to 200 mL of sample containing Cu(II) ion, then the solution was shaken for a specific time (15, 30, 60, 120, and 240 min) at room temperature to get the equilibrium time. The magnetic property of biocomposite facilitated the separation using an external magnetic field. The solution was passed 0.2 μm PVDF membranes for further observation. The filtrate was analyzed by inductively coupled plasma atomic emission spectrophotometer (ICP-AES JY2000 2, Horiba Jobin Yvon) to measure the Cu(II) ion remaining in solution. The experimental data was taken in duplicate. On the other hand, the performance of the reusability of biocomposite was also studied. Cu(II) ion-loaded RB-M and RB-NH_2 were released by shaking in 0.1 N HCl for 4 h. After washing with DI water, the regenerated RB-M and RB-NH_2 were used as adsorbent for the next run. The recycle usage of adsorbent was repeated four times. All samples were duplicated for treatment. The capacity of adsorption was determined applying the equation:

$$q_e = (C_o - C_e)\frac{V}{m} \quad (1)$$

where C_o (mg/L) is initial concentration of Cu(II) ion and C_e (mg/L) is the equilibrium concentration of Cu(II) ion. V (L) is the solution volume and m (g) is the amount of adsorbent.

5. Characterization

Surface morphology of sample was observed by field-emission scanning Eelectron microscopy (FE-SEM, JOEL JSM-6500F) and sputter coated by platinum before observation. Transmission electron microscopy (TEM) image was taken using a Hitachi H-800 transmission electron microscope (Japan). The X-Ray Fluorescence (XRF) observation by PANalytical/Minipal machine was used for detecting of elements. X-Ray diffraction (XRD) was investigated using a Rigaku D/MAX-B X-ray diffractometer equipped with Copper K-alpha (CuKα) radiation. The operation voltage worked at 40 kV and current for the machine worked at 100 mA. Autosorb-1 instrument was used to evaluate Brunauer-Emmet-Teller (BET) surface area equipped with nitrogen adsorption-desorption using a Quantachrome. The functional groups on the sample were investigated by using Fourier transform infrared spectrometry (FT-IR, Bio-rad, Digilab FTS-3500) in the wavelength range of 400-4,000 cm^{-1}.

6. Analysis

The amine contained on rice husk magnetic biocomposite was calculated by retro-titration method [21]. The RB-NH_2 (50 mg) was put in solution of 0.01 M HCl (25 mL) and shaken for 2 h at room temperature. After separation, the filtrate (10 mL) was titrated by 0.01 N NaOH. The amount of NaOH used is identified for amine concentration on sample. The calculation was by applying the equation:

$$C_{NH_2} = \left[\frac{(C_{HCl}\cdot V_{HCl}) - (5C_{NaOH}\cdot V_{NaOH})}{m_{sample}}\right] \quad (2)$$

where C_{HCl} is the HCl solution concentration (mmol/L), C_{NaOH} is the NaOH solution concentration (mmol/L); V_{HCl} and V_{NaOH} is the volume of HCl and NaOH used in the titration (L), respectively; weight of sample (g) is labeled as m_{sample}.

COD analysis was measured by titrimetric permanganate method; wastewater sample (100 mL) was treated with 6 N H_2SO_4 (1 mL) and followed by 0.01 N $KMnO_4$ (10 mL). The mixture in the flask was heated at boiling point and cooled to room temperature for 10 min and then 0.01 N of $H_2C_2O_4{\cdot}2H_2O$ (10 mL) was added to the flask. The mixture was titrated by 0.01 $KMnO_4$ until the solution changed to pink color. The blank solution used by DI water was also titrated by 0.01 $KMnO_4$. The titration continued until the purple color disappeared. The COD concentration was calculated by the following equation:

$$\mathrm{COD}\left(\frac{\mathrm{mg}}{\mathrm{L}}\right) = [(((a+b)\mathrm{x\ C\ KMnO_4}) - ((\mathrm{VxC})\mathrm{H_2C_2O_4}))] \times 8{,}000 \quad (3)$$

where: a is $KMnO_4$ volume for standard titration, b is $KMnO_4$ vol-

ume for sample titration, C $KMnO_4$ is $KMnO_4$ concentration (N), V $H_2C_2O_4$ is volume of $H_2C_2O_4$ (L) and C $H_2C_2O_4$ is concentration of $H_2C_2O_4$ (N), respectively.

The standard test method for filterable and nonfilterable matter in water was used for TSS. A well-mixed of sample was measured which filtered through a pre-weighed fiber filter. The filter was heated at 104±1 °C until constant mass and then weighed. The TSS was calculated by equation:

$$\mathrm{TSS}\left(\frac{\mathrm{mg}}{\mathrm{L}}\right)=\frac{(\mathrm{A}-\mathrm{B})\times 100}{\mathrm{C}} \quad (4)$$

where A is total dry weight of residue and filter (mg), B is dry weight of filter (mg), and C is sample volume (L). The dye intensity was tested by UV-Vis spectroscopy (V-550-JASCO), which worked on wavelength maximum color adsorption on sample.

RESULTS AND DISCUSSION

1. Characterization of Amine Rice Husk Magnetic Biocomposite

Delignification process on rice husk has an effect on its structure. The brown color of rice husk became gray and lighter (Fig. 1, inset). Basically, the rice husk is cellulosic material that has a complex structure. The morphology of RH, RH-D, RB-M and RB-NH_2 was observed by FE-SEM as shown in Fig. 1. The original RH has a surface (Fig. 1(a)), is still covered in lignin, hemicellulose, and other components that bind cellulose. After delignification, the shrink structure was formed (Fig. 1(b)). This is indicating loss of lignin and change of amorph structure into crystal form on RH. The NaOH as solvent facilitated the dissolving of lignin and hemicellulose [2].

The magnetic nanoparticle was grown on the surface of RH-D. The surface functionalization on biocomposite was an effect on the size of magnetic nanoparticle. The size becomes smaller about 30-50 nm (Fig. 1(d), inset) [22]. Amine groups have capability to prevent further growth of magnetic nanoparticle, and then initiate formation of new particles. On the other hand, the biocomposite without amine group produced magnetic nanoparticle in the range of 50-100 nm (Fig. 1(c), inset). From size measurement by TEM can be concluded that particle size of adsorbent was in nanoscale. Due to different size of magnetic nanoparticles, the surface area of RB-NH_2 significantly increased from 9.11 up to 19.45 $m^2\ g^{-1}$ measured by BET. In addition, amine content on RB-NH_2 was measured at about 2.9 mmol g^{-1}. Based on X-Ray, fluorescence was detected of Fe contained on RB-M and RB-NH_2 about 78.9% and 93%, respectively.

Delignification on RH was confirmed by changing structure from amorph (hemicellulose and lignin) to crystals (cellulose). The specific peaks of RH were identified at 2 tetha (°)=18.7° and 22.4° for amorph and crystalline structure, respectively. The crystallinity Index (CrI) of RH increased 20.87% after the delignification. The

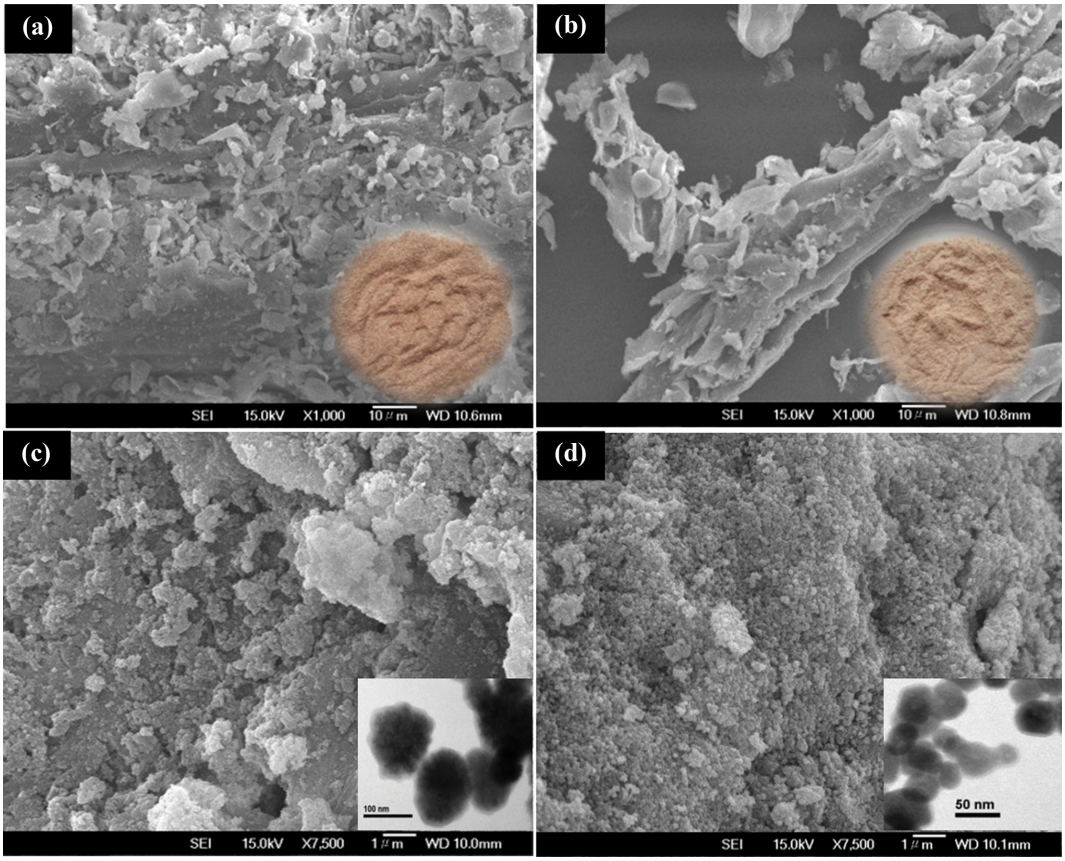

Fig. 1. FE-SEM images of (a) rice husk before treatment; (b) rice husk after treatment; (c) rice husk magnetic biocomposite without amine group (RB-M); (d) amine magnetic rice husk biocomposite (RB-NH_2).

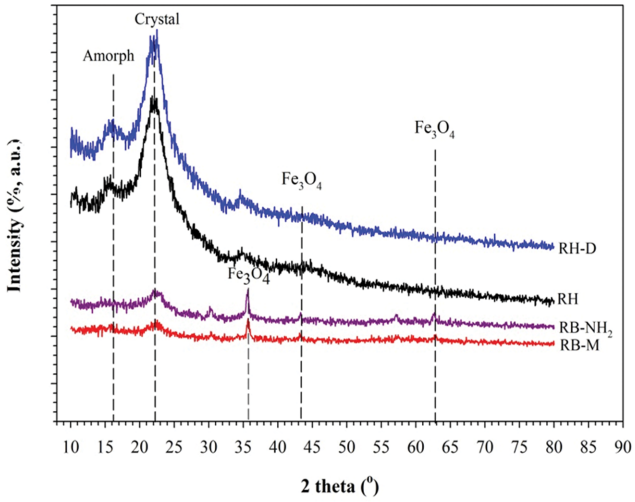

Fig. 2. X-Ray Diffraction (XRD) of rice husk (RH), RH after delignification (RH-D), rice husk magnetic biocomposite without amine (RB-M), and amine rice husk magnetic biocomposite ($RB-NH_2$).

NaOH successfully worked on RH [2] with effect of increasing intensity of the crystalline structure and reducing of amorph structure of polysaccharide [23]. The intensity of peaks of RH, RH-D, RB-M and $RB-NH_2$ by XRD is presented in Fig. 2. Physically, the RB-M and $RB-NH_2$ have a response to a magnetic field; specific types of peaks as magnetite at 36°, 43°, 63° were confirmed on XRD diffraction, which peaks are appropriate with crystalline magnetite (Fe_3O_4, JCPDS card 39-0664).

FT-IR spectra analysis was used to observe the functional groups on materials. The magnetic phase as Fe_3O_4 showed stretching of the Fe-O at 580 cm^{-1}. This peak was only found on RB-M and $RB-NH_2$. Amine groups also detected on $RB-NH_2$ at peak 1,540 cm^{-1}

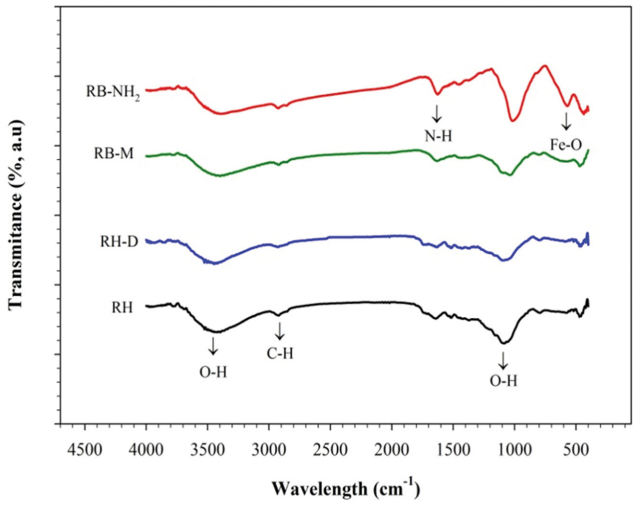

Fig. 3. FT-IR Spectra of rice husk (RH), RH after delignification (RH-D), rice husk magnetic biocomposite without amine (RB-M), and amine rice husk magnetic biocomposite ($RB-NH_2$).

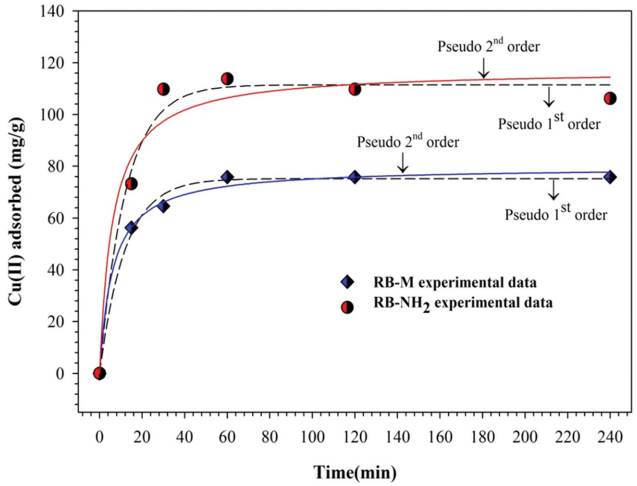

Fig. 4. The kinetic model of Cu(II) ion adsorbed onto RB-M and $RB-NH_2$ at room temperature. Initial concentration of Cu(II) of 50 mg L^{-1}, pH 7, shaking rate of 150 rpm.

for N-H bending vibration and at peak 950 cm^{-1} wavenumber reads for O-H bend (Fig. 3).

2. Kinetic Study of Cu(II) Ion Adsorption onto Amine Rice Husk Magnetic Biocomposites

Cu(II) ion kinetic adsorption on biocomposite was investigated with initial concentration of 50 mg L^{-1} at pH 6. The adsorption capacity of Cu(II) ion increased linearly up to 64.61 mg g^{-1} and 109.75 mg/g in 30 min, as shown in Fig. 4 for RB-M and $RB-NH_2$, respectively. Afterward, the Cu(II) ion adsorbed rate slowly increased and was constant to final of 75.84 mg g^{-1} and 113.75 mg g^{-1} reached after 60 min. At this moment, the equilibrium rate of adsorbent to capture Cu(II) ion occurred. The equilibrium time for Cu(II) adsorption on magnetic is similar with other reported research [24]. In addition, other type of adsorbent will take longer equilibrium time [25]. The adsorption capacity equilibrium data was fit to study adsorption model of Cu(II) using pseudo 1st order and pseudo 2nd order kinetic models [26]; the equations are:

$$\frac{dq_t}{dt} = k_1(q_e - q_t) \quad (5)$$

where q_e: Cu(II) ion adsorbed (mg g^{-1}) at equilibrium
q_t: Cu(II) ion adsorbed (mg g^{-1}) time
k_1: is the rate constant of adsorption (min^{-1}).

$$\frac{dq_t}{dt} = k_2(q_e - q_t)^2 \quad (6)$$

where q_e: the maximum adsorption capacity (mg g^{-1})
k_2: rate constant of the pseudo-2nd order equation (g mg^{-1} min^{-1})
q_t: the amount of Cu(II) adsorbed (mg g^{-1}).

The parameters of these two kinetic models (equilibrium value of q_e and rate constant) were calculated by using non-linear regression and the results are shown in Table 1. Based on higher number of coefficient correlation (r^2), the pseudo 2nd order and 1st order kinetic model fitted well for RB-M and $RB-NH_2$.

Table 1. The kinetic parameters of Cu(II) ion adsorption onto RB-M and RB-NH_2 at room temperature

Adsorbent	Kinetic model	Parameter constant	Value
RB-M	Pseudo 1st order	q_e (mg/g)	75.21
		k_1 (min)	0.084
		r^2	0.993
	Pseudo 2nd order	q_e (mg/g)	79.72
		k_2 (g/mg min)	0.002
		r^2	0.996
RB-NH_2	Pseudo 1st order	q_e (mg/g)	111.43
		k_1 (min)	0.081
		r^2	0.987
	Pseudo 2nd order	q_e (mg/g)	117.29
		k_2 (g/mg min)	0.001
		r^2	0.962

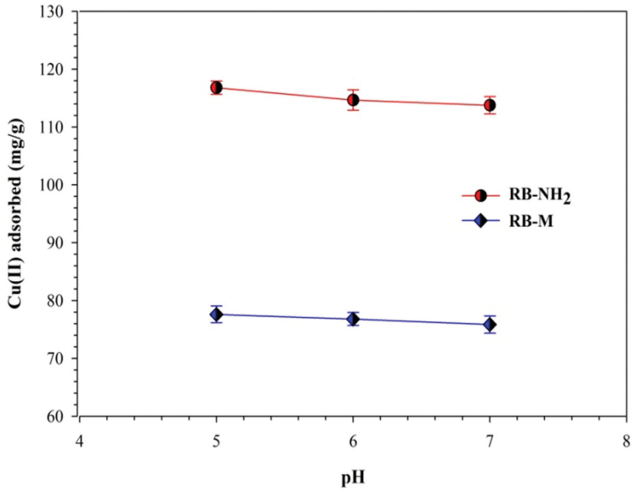

Fig. 5. The Cu(II) ion adsorbed in various pH onto RB-M and RB-NH_2. Cu(II) initial concentration of 50 mg L^{-1}, shaking rate of 150 rpm, 1 h.

The profile of adsorption of RB-NH_2 showed higher adsorption capacity than RB-M. This proved that amine group has a contribution to increase Cu(II) ion adsorption capacity about 48%. The amine groups play a role in absorption due to their ligand to capture ion as well as a smaller diameter of particle size [7]. So that, there is high surface area, high permeability and stable of mechanical and thermal properties of RB-NH_2.

3. The pH Solution Effect on Cu(II) Ion Adsorption, Chemical Oxygen Demand (COD), Total Suspended Solid (TSS), and Dye Adsorption onto Amine Functionalized Rice Husk Magnetic Nanoparticle Biocomposite

The pH equilibrium (pH_e) of a solution is very important for metal ion removal and also to predict the main driving force for adsorption. This effect of pH on adsorption is related to protonation or deprotonation of adsorbent active side [27] and degree of ionization and species type of ion [28]. This research only observed adsorption in the pH range of 5-7. For low pH at 1-4, the iron content on biocomposite will release to the solution. On the other hand, working at higher of pH, Cu(II) ion will precipitate on base condition to form $Cu(OH)_2$. The pH effect on Cu(II) ion adsorption on RB-M and RB-NH_2 as adsorbent can be seen in Fig. 5. It shows higher adsorption capacity at pH 5, the RB-M and RB-NH_2 with adsorption capacity about 77.6 mg g^{-1} and 116.80 mg g^{-1}, respectively. Interestingly, the adsorption capacity at pH 5-7 is quite small. In other words, the active site is stable at pH 5-7. In contrast, RB-NH_2 again has shown 50% higher reactivity than RB-M for all range of pH. This condition also proved that amine groups on the surface of particle are quite stable.

The surface stability of RB-NH_2 due to formation of positive charged (-NH_3^+). The water solubility of amines is enhanced by hydrogen bonding, including these lone electron pairs, then interaction occurred with Cu(II) ion in solution as shown in Fig. 6. Based on Hard-Soft Acids and Bases (HSAB) theory, the RB-NH_2 is hard base, which has covalent complexes interaction with Cu(II) as soft acid. It proved cationic amine group formation in range of pH 2-7 [7,29]. On the other hand, the capability of biocomposite is limited to capturing Cu(II) ion, so that there still is a vacancy of active site as negative charge to interact with positive charge of molecules in the solution.

In the case RB-M as magnetite has point zero charge (P_{ZC}) at 5.5 of pH, so the surface charge of RHB-M is below P_{ZC} on positive charged and over P_{ZC} in negative charged [12]. In this condi-

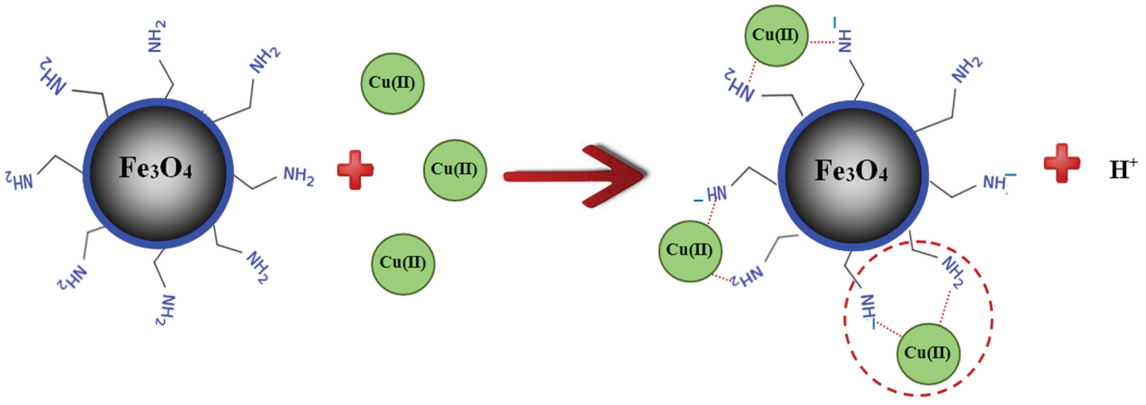

Fig. 6. The Cu(II) ion adsorption mechanism of amine rice husk magnetic nanoparticle biocomposite (RB-NH_2).

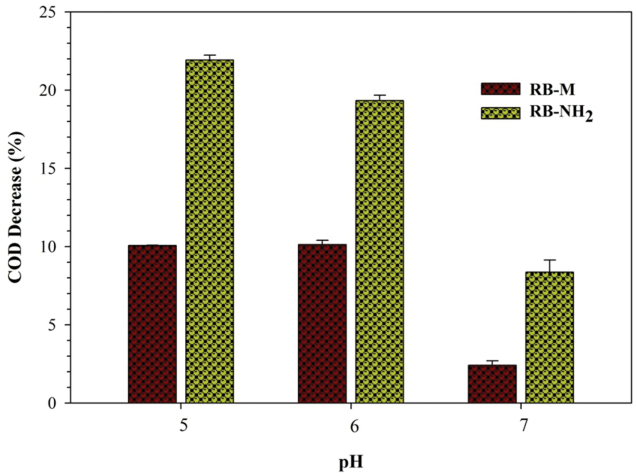

Fig. 7. The COD reduction in various pH onto RB-M and RB-NH_2 as adsorbent in wastewater containing Cu(II) ion of 50 mg L^{-1}, shaking rate of 150 rpm, 1 h.

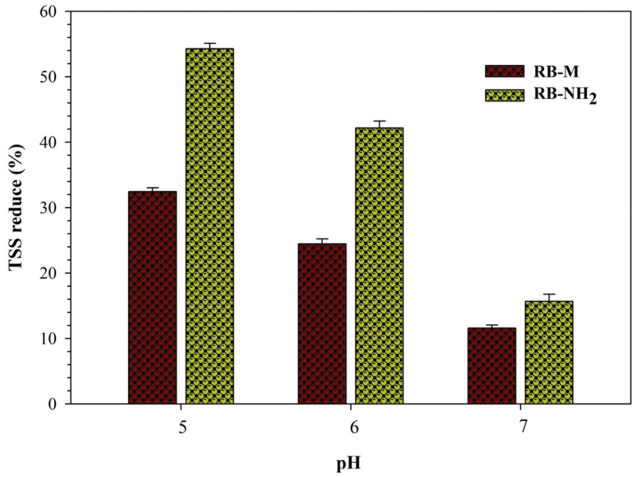

Fig. 8. TSS reduction in various of pH onto RB-M and RB-NH_2 as adsorbent in wastewater containing Cu(II) ion of 50 mg L^{-1}, shaking rate of 150 rpm, 1 h.

tion, the RB-M surface charge will increase due to negative charged formation and electrostatic interaction to capture Cu(II) ion. The protonation of Cu(II) ion in the range of pH facilitates electrostatic and complexation mechanism to have good capability for adsorption [30].

Another parameter of quality of water is COD. Its concentration is also influenced by pH solution, then is related to adsorbent surface charge, degree of ionization, stability and color intensity of the compounds in solution [31]. Fig. 7 shows COD reduction at various pH with initial concentration on COD of 998 mg/L. The higest reduction of COD occurred at pH of 5 with value of 10% and 22% for RB-M and RB-NH_2, respectively. For higher pH, COD will decrease and lower adsorption occurs due to an increased diffusion of organic ions as well as the abundance of OH- ions; this causes competition between organic molecules and the adsorbent surface charge [32]. In addition, when organic molecules are positively charged, they have electrostatic interaction with negative charge of the adsorbent. This result accords with another study, COD reduction also incrased by adsorbent made from bagasse at low pH [33].

Another parameter that has an effect on wastewater treatment is TSS, due to surface positive charge of adsorbent. The positive charge is able to absorb negative charges of suspended surface particles, then repulsive interaction force occurs with suspended particles. The suspended particles in solution can be neutralized with positive charge from adsorbent, then the solution becomes stable. Fig. 8 shows the TSS reduction during adsorption process in the presence of RB-M and RB-NH_2 with initial concentration of TSS of about 355 mg L^{-1}. At low pH the TSS reduction percentage is higher than other pH, the reducing number of TSS for RB-M and RB-NH_2 at pH 5 is 32.44% and 54.37%, respectively. The degradation process of organic and inorganic compounds takes place optimally at acidic solution, causing the suspended substances to be redissolved in large quantities, which will increase the percentage of TSS reduction [34].

The color change of wastewater was also observed in this research; the profile of reducing of dye during adsorption is shown in Fig. 9.

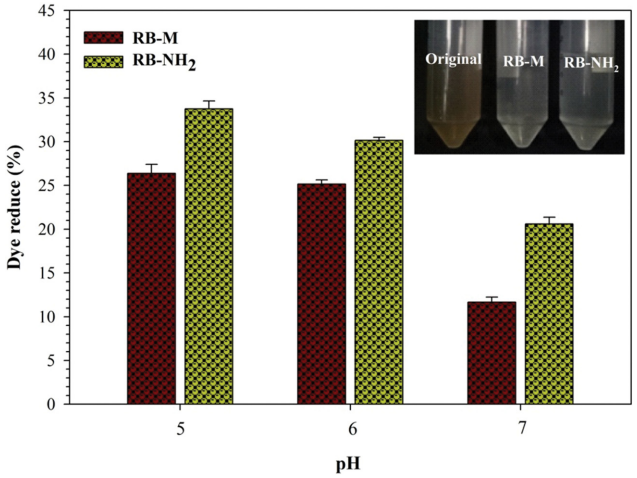

Fig. 9. Dye reduction in various of pH onto RB-M and RB-NH_2 as adsorbent in wastewater containing Cu(II) ion of 50 mg L^{-1}, shaking rate of 150 rpm, 1 h.

The high dye reduction for RB-M and RB-NH_2 occurred at pH 5 about 26.38% and 33.74% for RB-M and RB-NH_2, respectively. The initial dye concentration was 1.363 PtCo. Reduction color for dye was observed before adsorption and after adsorption by using RB-M and RB-NH_2 (Fig. 6(b), inset). It is clear that the original color (brown) disappears, becoming a clear solution after adsorption. The decrease of dye intensity in solution is probably due to protonation, and that would be the specific cause for the enhancement of electrostatic interaction between the negatively charged anions in the dye molecules and the positively charged of adsorbent active site [35].

In fact, the hydrogen ion concentration in a solution with pH of 5 is higher and this causes the hydrogen ions to compete with another contaminant for the active site. Hence, the presence of hydrogen ions can reduce the adsorption capacity of dye. The pH of the adsorbate affects the electrostatic force of the ion to relate to the func-

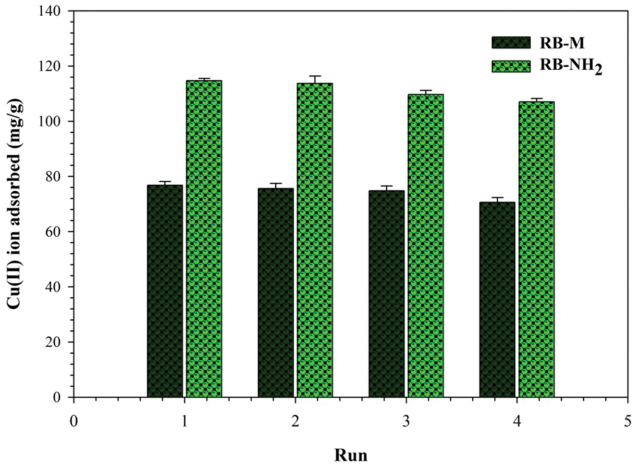

Fig. 10. Repetition of the adsorbent in the adsorption for RB-M and RB-NH_2 process with a sample volume of 200 mL, pH 5, shaking rate of 150 rpm, 60 min.

tional groups on the adsorbent [36].

4. Reusability of Amine Rice Husk Biocomposite for Cu(II) Ion Adsorption

The important thing related to economic and efficiency factor for material is being able to reduce secondary waste. The magnetic properties of adsorbent also facilitate reusability and easy separation. After one cycle experiments, the adsorbent is used again for the next adsorption after a thorough washing process. After 4th repetition, the adsorption capacity of Cu(II) ion decreased only 8% for RB-M and 6.6% for RB-NH_2 (Fig. 10). The adsorbent efficiency of those adsorbents during fourth cycle was 92% and 94.6% for RB-M and RB-NH_2, respectively. This performance is similar to Pb(II) ion removal using amine magnetic biocomposite [7].

The concentration of Cu(II) ion absorbed decreased after four times used. Based on observation of amine concentration and H^+ ion, there is a decreasing number of functional groups for each step around 1-8%; this could be followed by decreasing of adsorption capacity. This could be possible because of the reduced concentration of H^+ ions during washing step. HCl was used for washing where the Cu(II) will bind with Cl^- to become $CuCl_2$. The evaluated adsorbent performance shows a good performance and still effective for reuse as adsorbent.

CONCLUSION

The synthesis of amine functionalized on biocomposite using rice husk cellulose with magnetic nanoparticles was successfully synthesized by solvothermal method. The cellulose based biocomposite enhances the value added of biomass. The biocomposite has good on Cu(II) ion adsorption, reduction of COD, TSS and dye in waste water treatment. The biocomposite material was tested for reusability and that showed it only reduces performance slightly. The multiple effects of amine rice husk magnetic biocomposite on wastewater contaminants leads to becoming a candidate material to be developed and applied in a wide range of waste water treatment applications.

ACKNOWLEDGEMENTS

The authors wish to thank the Ministry of Education, Culture, Research and Technology (Kemendikbudristek) Republic of Indonesia with grant number 031/E4.1/AK.04.PT/2021.

REFERENCES

1. Y. Zou and T. Yang, in *Rice Bran and Rice Bran Oil*, edited by L.-Z. Cheong and X. Xu, AOCS Press (2019).
2. E. Menya, P. W. Olupot, H. Storz, M. Lubwama, Y. Kiros and M. J. John, *J. Therm. Anal. Calorim.*, **139**, 1681 (2020).
3. N. Bisht, P. C. Gope and N. Rani, *J. Mechanical Behavior Mater.*, **29**, 147 (2020).
4. M. Dominic, R. Joseph, P. M. Sabura Begum, B. P. Kanoth, J. Chandra and S. Thomas, *Carbohydr. Polym.*, **230**, 115620 (2020).
5. H. Keshavarz, A. Khavandi, S. Alamolhoda and M. R. Naimi-Jamal, *New J. Chem.*, **44**, 8232 (2020).
6. P. Kaur, P. Kaur and K. Kaur, *J. Cleaner Production*, **244**, 118699 (2020).
7. I. F. Nata, D. R. Wicakso, A. Mirwan, C. Irawan, D. Ramadhani and Ursulla, *J. Environ. Chem. Eng.*, **8**, 104339 (2020).
8. A. Daem, P. Sergeant, L. Dupré, S. Chaudhuri, V. Bliznuk and L. Kestens, *Materials*, **13**, 4361 (2020).
9. X. Gao, M. Zhai, W. Guan, J. Liu, Z. Liu and A. Damirin, *ACS Appl. Mater. Interfaces*, **9**, 3455 (2017).
10. G. R. Rodrigues, C. López-Abarrategui, I. de la Serna Gómez, S. C. Dias, A. J. Otero-González and O. L. Franco, *Int. J. Pharm.*, **555**, 356 (2019).
11. M. Ariannezhad, D. Habibi, S. Heydari and V. Khorramabadi, *Korean J. Chem. Eng.*, **38**, 1510 (2021).
12. I. F. Nata, N. S. El-Safory and C.-K. Lee, *Appl. Mater. Interfaces*, **3**, 3342 (2011).
13. G. K. Sarma, S. Sen Gupta and K. G. Bhattacharyya, *Environ. Sci. Pollut. Res.*, **26**, 6245 (2019).
14. N. N. Malinga and A. L. L. Jarvis, *Korean J. Chem. Eng.*, **37**, 1915 (2020).
15. Y. Yang, Z. Zheng, W. Ji, J. Xu and X. Zhang, *J. Hazard. Mater.*, **395**, 122686 (2020).
16. H. T. Ha, T. D. Minh, H. M. Nguyet and A. K. Sharma, *Korean J. Chem. Eng.*, **38**, 22 (2021).
17. K. Qiao, W. Tian, J. Bai, L. Wang, J. Zhao, Z. Du and X. Gong, *J. Taiwan Inst. Chem. Eng.*, **97**, 227 (2019).
18. J.-H. Wu and C.-Y. He, *Chromatographia*, **82**, 1151 (2019).
19. T. Kim, D. Yang, J. Kim, H. Musaev and A. Navarro, *Trends Chromatog*, **8**, 97 (2013).
20. I. F. Nata, A. Mirwan, D. R. Wicakso, C. Irawan, M. D. Isnaini and R. Fitriani, *IOP Conference Series: Earth and Environ. Sci.*, **506**, 012006 (2020).
21. B. Pi-Boleda, M. Bouzas, N. Gaztelumendi, O. Illa, C. Nogués, V. Branchadell, R. Pons and R. M. Ortuño, *J. Mol. Liq.*, **297**, 111856 (2020).
22. C. Irawan, I. F. Nata and C.-K. Lee, *J. Environ. Chem. Eng.*, **1**, 1245 (2019).
23. L. Ghali, S. Msahli, M. Zidi and F. Sakli, *Mater. Lett.*, **63**, 61 (2009).
24. N. Ghaemi, S. S. Madaeni, P. Daraei, H. Rajabi, S. Zinadini, A. Aliza-

deh, R. Heydari, M. Beygzadeh and S. Ghouzivand, *Chem. Eng. J.*, **263**, 101 (2015).
25. Z. Liu, X. Li, P. Zhan, F. Hu and X. Ye, *Sep. Purif. Technol.*, **206**, 199 (2018).
26. J. Qu, X. Tian, Z. Jiang, B. Cao, M. S. Akindolie, Q. Hu, C. Feng, Y. Feng, X. Meng and Y. Zhang, *J. Hazard. Mater.*, **387**, 121718 (2020).
27. V. Aghazadeh, S. Barakan and E. Bidari, *J. Mol. Struct.*, **1204**, 127570 (2020).
28. S. Periyasamy, V. Gopalakannan and N. Viswanathan, *Carbohydr. Polym.*, **174**, 352 (2017).
29. Y.-M. Hao, C. Man and Z.-B. Hu, *J. Hazard. Mater.*, **184**, 392 (2010).
30. C. Irawan, M. D. Putra, H. Wijayanti, R. Juwita, Y. Meliana and I. F. Nata, *Molecules*, **26**, 5867 (2021).
31. S. Lucinaldo, C. Luciano, J. Fransisco, S. Mateus, A. Josy, D. Roosevelt and C. Edson, *Open Chem.*, **13**, 801 (2015).
32. A. Al Bsoul, M. Hailat, A. Abdelhay, M. Tawalbeh, I. Jum'h and K. Bani-Melhem, *Sci. Total Environ.*, **688**, 1327 (2019).
33. Y. Pan, Y. Zhu, Z. Xu, R. Lu, Z. Zhang, M. Liang and H. Liu, presented at *5th Inter. Conference on Bioinformatics and Biomedical Engineering*, 1 (2011).
34. E. M. Cuerda-Correa, M. F. Alexandre-Franco and C. Fernández-González, *Water*, **12**(1), 102 (2020).
35. R. Sivashankar, A. Sathya and V. Sivasubramanian, *Ecotoxicol. Environ. Saf.*, **121**, 149 (2015).
36. T. Y. Ying, A. A. A. Raman, M. M. Bello and A. Buthiyappan, *Korean J. Chem. Eng.*, **37**, 2179 (2020).